

## Third-order nonlinearities in silicon at telecom wavelengths

M. Dinu,<sup>a)</sup> F. Quochi, and H. Garcia

*Bell Laboratories, Lucent Technologies, 101 Crawfords Corner Road, Holmdel, New Jersey 07733*

(Received 10 June 2002; accepted 7 March 2003)

The two-photon absorption coefficient and Kerr coefficient of bulk crystalline silicon are determined near the telecommunication wavelengths of 1.3 and 1.55  $\mu\text{m}$  using femtosecond pulses and a balanced Z-scan technique. A phase shift sensitivity of the order of 1 mrad is achieved, enabling the accurate measurement of third-order nonlinear coefficients at fluences smaller than 100  $\mu\text{J}/\text{cm}^2$ . From the two-photon absorption coefficient ( $\beta \sim 0.8 \text{ cm}/\text{GW}$ ) and the Kerr coefficient ( $n_2 \sim 4 \times 10^{-14} \text{ cm}^2/\text{W}$ ) at a wavelength  $\lambda = 1.54 \mu\text{m}$ , a value  $F \sim 0.35$  for the nonlinear figure of merit for all-optical switching is determined. © 2003 American Institute of Physics.  
[DOI: 10.1063/1.1571665]

In current optical networks, an increasing variety of optical waveguide devices implement functions such as modulation, wavelength multiplexing and demultiplexing, or wavelength add-drop, at ever higher data rates and optical intensities. While the nonlinear optical properties of the materials will ultimately limit the performance of passive (linear) optical devices, in the context of future applications such as all-optical switching, all-optical regeneration, or optical gating, it is desirable to use materials with large ultrafast nonlinearities. Distinguishing between the real (refractive) and the imaginary (absorptive) part of the third-order nonlinear coefficient  $\chi^{(3)}$  may be important depending on the type of all-optical function to be implemented. Single beam measurement techniques such as the Z-scan<sup>1</sup> technique and spectrally resolved pump-probe measurements<sup>2</sup> have been used to determine and distinguish between the real and imaginary parts of the nonlinear susceptibility. While spectrally resolved pump-probe measurements benefit from extremely high sensitivity<sup>2</sup> and are insensitive to structural sample inhomogeneities, the Z-scan technique is a simple and robust single beam measurement which enables direct and accurate determination of nonlinear coefficients. Variations of the Z-scan technique have been used to determine small linear absorption coefficients by measuring thermal lensing effects due to an intense laser beam.<sup>3</sup> Linear optical effects may therefore limit the sensitivity floor of the Z-scan technique when measuring weak nonlinearities which require the use of high power beams or high energy per pulse; in this case thermal effects, free carrier nonlinearities, or even artifacts in the Z-scan trace due to sample structural inhomogeneities<sup>4</sup> can obscure or mimic contributions from material nonlinearities.

In this letter we report Z-scan measurements of the two-photon absorption coefficient  $\beta$  and the Kerr coefficient  $n_2$  in bulk samples of silicon at telecom wavelengths, where little data on the nonlinear optical coefficients of silicon are available,<sup>5</sup> in spite of the appeal of silicon as a material for optical integrated devices,<sup>6</sup> stemming from its small absorption and the widespread use and maturity of silicon processing techniques.

In the Z-scan technique (Fig. 1), a sample of thickness  $L$  is translated through the focus of a beam with a Gaussian spatial profile, and the transmission through an aperture behind the sample is measured as a function of the longitudinal coordinate  $z$ . In the case of open aperture Z-scan (aperture transmission  $S = 1$ ), and for pulses with Gaussian temporal dependence, the total time-integrated transmission is related to the peak on-axis intensity  $I_0$  by

$$T_{\text{op}}(z) = 1 - \frac{1}{2\sqrt{2}} \frac{\beta I_0 L}{1+x^2}, \quad (1)$$

where  $x = z/z_0$ , the confocal parameter is  $z_0 = kw^2$ , with  $k = 2\pi/\lambda$  the free space wave vector, and  $w$  is the  $(1/e)$  intensity beam waist. In closed aperture ( $S < 1$ ) Z-scan, due to the nonlinear focusing of the beam, the transmission through the aperture displays a characteristic peak-valley shape, which under the approximation of small refractive and absorption changes depends on the coordinate  $z$  as<sup>7,8</sup>

$$T_{\text{cl}}(z) \cong 1 + \frac{4x \langle \Delta \Phi_0 \rangle}{(1+x^2)(9+x^2)} - \frac{\beta I_0 L}{2\sqrt{2}} \frac{(3-x^2)}{(1+x^2)(9+x^2)}. \quad (2)$$

The time-averaged peak on-axis phase change  $\langle \Delta \Phi_0 \rangle$  (at the center of the Gaussian beam profile) is a function of the nonlinear refractive coefficient  $n_2$  and of the aperture transmission  $S$  and can be approximated as

$$\langle \Delta \Phi_0 \rangle \cong \frac{1}{\sqrt{2}} (1-S)^{0.25} k L n_2 I_0. \quad (3)$$

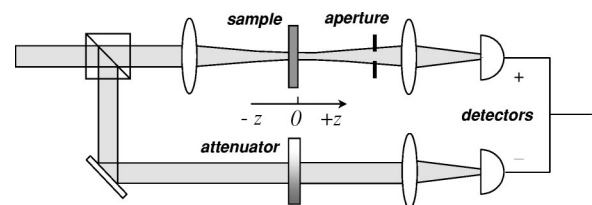


FIG. 1. Schematic of balanced Z-scan experimental setup.

<sup>a)</sup>Electronic mail: mdinu@lucent.com

In the case of small nonlinear phase shifts ( $\langle \Delta \Phi_0 \rangle \ll \pi$ ), the peak-to-valley transmission change in a Z-scan trace for purely refractive nonlinearities is<sup>1</sup>  $\Delta T_{p-v} \cong 0.406 \langle \Delta \Phi_0 \rangle$ . Thus, both the magnitude and sign of the real and imaginary part of the third-order nonlinearity can be determined directly from the Z-scan traces. Quantitatively accurate results require the knowledge of the peak intensity at the focus, which is calibrated using the measured focal spot size and can also be determined from the confocal parameter.

The sensitivity of the single-beam Z-scan is typically limited by laser source noise (with intensity fluctuations typically of order  $10^{-2}$ ) and, because the sample is translated through the focus of the beam, by scatter from sample inhomogeneities. In order to reduce the measurement noise well below the fluctuations of the laser source, we employ balanced detection<sup>9</sup> using a balanced Nirvana 1607 photodetector followed by lock-in amplification. Ultrashort pulses from either a commercial fiber mode-locked laser ( $\lambda = 1.54 \mu\text{m}$ , pulse width  $t_p = 220$  fs, 10 MHz repetition rate) or from a tunable optical parametric oscillator (OPO) pumped by a mode-locked Ti:sapphire laser ( $\lambda = 1.27 \mu\text{m}$  or  $\lambda = 1.54 \mu\text{m}$ , pulse width  $t_p = 130$  fs, and 76 MHz repetition rate) were focused on the samples using a lens with focal length  $f = 75$  mm. The pulse fluence is determined using the measured Gaussian beam waist; the shapes of the Z-scan traces from Eqs. (1) and (2) provide a consistency check for the beam waist value. Fresnel losses on the front sample surface are taken into account when determining the intensity inside the sample. The use of ultrashort pulse sources with low ( $< 1$  nJ) energy per pulse minimizes thermal effects<sup>4</sup> and free carrier generation.<sup>10</sup> We characterized the pulses via two-photon autocorrelation in a silicon avalanche photodiode, and estimated the pulse durations either by assuming a  $\text{sech}^2$  pulse shape in the case of the OPO or by retrieving the temporal profile from the autocorrelation versus delay in the case of the fiber laser. For well-behaved pulses this procedure yields fairly accurate pulse shapes, leading to deviations from the actual pulse only in the wings of the pulse.<sup>11,12</sup> The non-Gaussian pulse shape was taken into account (where applicable) by replacing the  $\sqrt{2}$  factor in the denominator of Eqs. (1) and (2) with the appropriate temporal integral. The estimated errors on the nonlinear coefficients are therefore due mainly to uncertainties in the pulse peak intensity originating from uncertainties in the retrieved pulse shape and duration.

For all measurements, Z-scans were taken at low intensity and subtracted from the high-intensity scans in order to account for inhomogeneities in the sample.<sup>1</sup> This ensures a detectable change in transmission  $\Delta T < 10^{-3}$  for both the open and the closed aperture scans, comparable to the sensitivity offered by the occultation or EZ-scan method.<sup>13</sup> Z-scan measurements were performed at several incident intensities on two bulk silicon samples, with sample thickness  $L = 480 \mu\text{m}$ , resistivity ( $n$  and  $p$  type)  $\rho \sim 10 \Omega \text{ cm}$ , and crystallographic orientations along the  $\langle 110 \rangle$  or  $\langle 111 \rangle$  directions. Figure 2 shows typical open and closed aperture Z-scan traces for the Si  $\langle 110 \rangle$  sample; the normalized closed aperture trace  $T_{cl}(z)/T_{op}(z)$  is shown in Fig. 2(c). Maximum changes in transmission of less than 1% are observed with good

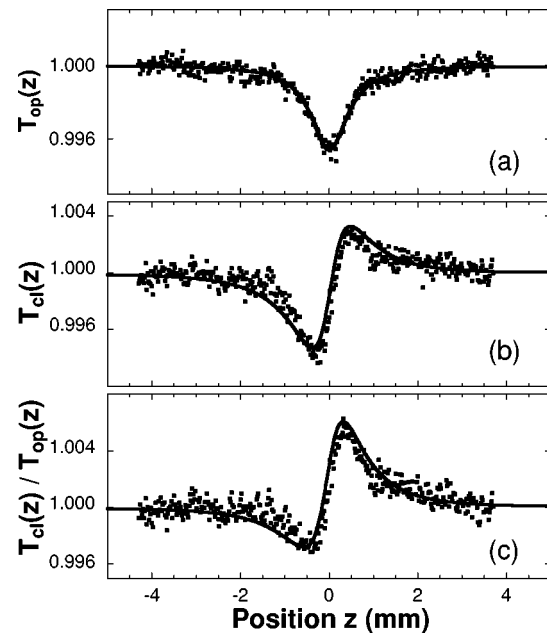


FIG. 2. Transmission vs position  $z$  of  $\langle 110 \rangle$  silicon for (a) open aperture and (b) closed aperture ( $S=0.40$ ) Z-scans for an incident peak intensity  $I_0 = 0.7 \text{ GW/cm}^2$ . The normalized transmission of the closed aperture trace is shown in (c). The dots are experimental points and the lines are fits to the data yielding  $\beta = 0.79 \text{ cm/GW}$  and  $n_2 = 4.5 \times 10^{-14} \text{ cm}^2/\text{W}$ .

signal-to-noise ratio. The noise on the Z-scan traces is less than 6% and is due principally to the surface inhomogeneities of the samples. The nonlinear absorption term accentuates the minimum and depresses the maximum in the closed aperture Z-scan trace in Fig. 2(b) as compared to the purely refractive case, where the trace is antisymmetric with respect to the focal plane. The normalized closed aperture trace is typically well approximated by the pure refractive term in Eq. (2).

At the fluences used in these experiments, on the order of  $100 \mu\text{J/cm}^2$ , the contributions from free carriers and thermal effects to the nonlinear refractive index were estimated<sup>10,14</sup> to be less than  $10^{-17}$  and  $10^{-16} \text{ cm}^2/\text{W}$ , respectively. At higher fluences, the free carrier contribution to the nonlinear refractive index can become comparable in magnitude to the ultrafast (electronic) nonlinearity,<sup>15</sup> and its sign may also vary with wavelength, leading to either an underestimate or overestimate of the Kerr coefficient depending on wavelength and pulse fluence. To further exclude free carrier effects, in time-resolved pump-probe measurements the differential transmission signal is verified to be practically instantaneous, limited only by the duration of the femtosecond laser pulses, and the magnitude of the two-photon absorption peak is consistent with the values of the two-photon absorption coefficient extracted from the time-integrated Z-scan measurements.

The two-photon absorption  $\beta$  and Kerr coefficient  $n_2$  can be determined directly from the open aperture and closed aperture transmission changes  $\Delta T$  and  $\Delta T_{p-v}$ , or from theoretical fits such as those shown in Fig. 2. The results are summarized in Table I for the two silicon substrates. For comparison, we also determined  $n_2$  and  $\beta$  for a GaAs sample at the two wavelengths, leading to results comparable to those reported in the literature.<sup>10,16</sup> The errors on the measured values are estimated to be  $\pm 15\%$ , determined mainly

TABLE I. Measured two-photon absorption and Kerr coefficients for silicon and gallium arsenide. The relative errors are estimated as  $\pm 15\%$ .

Material	$\lambda = 1.54 \mu\text{m}$			$\lambda = 1.27 \mu\text{m}$		
	$n_2$ (cm <sup>2</sup> /W)	$\beta$ (cm/GW)	$F$	$n_2$ (cm <sup>2</sup> /W)	$\beta$ (cm/GW)	$F$
Si <110>	$0.45 \times 10^{-13}$	0.79	0.37	$0.26 \times 10^{-13}$	0.74	0.28
Si <111>	$0.43 \times 10^{-13}$	0.88	0.32	...	...	...
GaAs	$1.59 \times 10^{-13}$	10.2	0.10	$-0.79 \times 10^{-13}$	15.1	0.04

by uncertainties in the pulse shapes. Within experimental error, the nonlinear coefficients of silicon are independent of the crystal orientation and only weakly dependent on wavelength. The two-photon transition in an indirect gap material such as silicon can be presumed to be phonon mediated. Unlike the class of direct band gap zinc blende semiconductors, where theoretical estimates and scaling rules for two-photon absorption and Kerr refraction are available,<sup>17,18</sup> no theoretical determination or scaling rules exist for phonon-mediated multiphoton absorption and for the dispersion of the associated nonlinear refraction.

Figure 3 shows the changes in transmission due to nonlinear absorption  $\Delta T$  and refraction  $\Delta T_{p-v}$  plotted against incident power for the two silicon samples. A linear dependence is evident in the plots, with the correct scaling for two-photon absorption. From the measured values for two-photon absorption and nonlinear refraction, we can extract the nonlinear figure of merit  $F = n_2 / (\beta\lambda)$ . In all-optical devices relying on optical nonlinearities, such as nonlinear directional couplers, a figure of merit  $F > 2$  is required.<sup>19</sup> The figure of merit can be calculated directly from the ratio of transmission changes in the Z-scan traces for  $S = 0.40$

$$F \cong \frac{\Delta T_{p-v}|_{\text{closed}}}{4.489 \Delta T|_{\text{open}}} \quad (4)$$

It is worth noting that this expression is insensitive to the exact temporal profile of the laser pulses, which is normalized out of the ratio. Values for the figure of merit  $F$  are listed in Table I. While the values for GaAs are consistent with previous results,<sup>10</sup> in the case of silicon we extract a

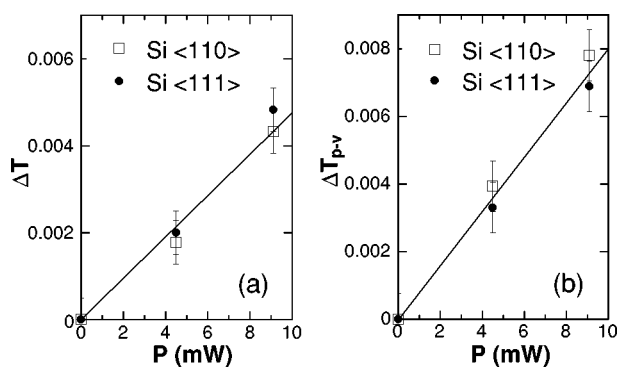


FIG. 3. Peak transmission change vs average incident power for open aperture Z scan (a) and peak-to-valley transmission for closed aperture Z-scan for <110> and <111> silicon at  $1.54 \mu\text{m}$ . The solid lines are fits to a linear dependence, as would be expected for a third-order nonlinearity.

figure of merit smaller by a factor of  $\sim 3$  compared with the only previously published data.<sup>5</sup> The value of the nonlinear figure of merit is an important parameter for all-optical switching devices, where nonlinear absorption leads not only to a decrease in throughput, but also to a dramatic increase in switching power and to a degradation of the cross-talk and extinction ratio.<sup>19</sup>

In conclusion, we determined the third-order absorptive and refractive nonlinearities of silicon at the wavelengths of 1.27 and  $1.54 \mu\text{m}$  in low-fluence Z-scan measurements, under conditions where thermal and free-carrier contributions to the nonlinear refraction and absorption are negligible. The nonlinear coefficients and the nonlinear figure of merit are important material parameters both for the design of passive silicon optical waveguide devices and for the potential of silicon as a nonlinear material for all-optical processing and switching.

The authors thank F. H. Baumann and J. Perna for help with the preparation of the samples and acknowledge useful discussions with G. D. Boyd.

- <sup>1</sup>M. Sheik-Bahae, A. A. Said, T.-H. Wei, D. J. Hagan, and E. W. Van Stryland, IEEE J. Quantum Electron. **26**, 760 (1990).
- <sup>2</sup>I. Kang, T. Krauss, and F. Wise, Opt. Lett. **22**, 1077 (1997).
- <sup>3</sup>S. S. Gupte, A. Marcano O., R. D. Pradhan, C. F. Desai, and N. Melikechi, J. Appl. Phys. **89**, 4939 (2001).
- <sup>4</sup>R. de Nalda, R. del Cosco, J. Requejo-Isidro, J. Olivares, A. Suarez-Garcia, J. Solis, and C. N. Alfonso, J. Opt. Soc. Am. B **19**, 289 (2002).
- <sup>5</sup>H. K. Tsang, C. S. Wong, T. K. Liang, I. E. Day, S. W. Roberts, A. Harpin, J. Drake, and M. Ashgari, Appl. Phys. Lett. **80**, 416 (2002).
- <sup>6</sup>A. G. Rickman and G. T. Reed, IEE Proc.-J: Optoelectron. **141**, 391 (1994).
- <sup>7</sup>B. K. Rhee, J. S. Byun, and E. W. V. Stryland, J. Opt. Soc. Am. B **13**, 2720 (1996).
- <sup>8</sup>Y. Choi, J.-H. Park, M. R. Kim, W. Je, and B. K. Rhee, Appl. Phys. Lett. **78**, 856 (2001).
- <sup>9</sup>T. D. Krauss and F. Wise, Appl. Phys. Lett. **65**, 1739 (1994).
- <sup>10</sup>T. G. Ulmer, R. K. Tan, Z. Zhou, S. E. Ralph, R. P. Kenan, and C. M. Verber, Opt. Lett. **24**, 756 (1999).
- <sup>11</sup>J. Peatross and A. Rundquist, J. Opt. Soc. Am. B **15**, 216 (1998).
- <sup>12</sup>J.-H. Chung and A. M. Weiner, IEEE J. Sel. Top. Quantum Electron. **7**, 656 (2001).
- <sup>13</sup>T. Xia, D. J. Hagan, M. Sheik-Bahae, and E. W. Van Stryland, Opt. Lett. **19**, 317 (1994).
- <sup>14</sup>M. Lax, J. Appl. Phys. **48**, 3919 (1977).
- <sup>15</sup>B. R. Bennett, R. A. Soref, and J. A. D. Alamo, IEEE J. Quantum Electron. **26**, 113 (1990).
- <sup>16</sup>A. Villeneuve, C. C. Yang, G. I. Stegeman, C. N. Ironside, G. Scelsi, and R. M. Osgood, IEEE J. Quantum Electron. **30**, 1172 (1994).
- <sup>17</sup>B. S. Wherrett, J. Opt. Soc. Am. B **1**, 67 (1984).
- <sup>18</sup>M. Sheik-Bahae, D. J. Hagan, and E. W. Van Stryland, Phys. Rev. Lett. **65**, 96 (1990).
- <sup>19</sup>K. W. DeLong, K. B. Rochford, and G. I. Stegeman, Appl. Phys. Lett. **55**, 1823 (1989).